This article has been accepted for publication in a future issue of this journal, but has not been fully edited. Content may change prior to final publication. Citation information: DOI 10.1109/TSG.2018.2880654, IEEE Transactions on Smart Grid

Joint Energy Scheduling and Water Saving in Geo-Distributed Mixed-Use Buildings

Chuan Pham*, Nguyen H. Tran¶†, Shaolei Ren‡, Choong Seon Hong†, Kim Khoa Nguyen*, Mohamed Cheriet*
*Synchromedia - École de Technologie Suprieure, Université du Québec, H3C1K3, Canada,
¶ School of Information Technologies, The University of Sydney, NSW, Australia.
†Department of Computer Science and Engineering, Kyung Hee University, Korea,
‡Department of Electrical & Computer Engineering, University of California at Riverside, USA,

***Abstract*—Coordinated approaches between datacenter and non-datacenter loads in buildings to achieve energy efficiency have been widely studied in recent years. However, the coordination-enabled mechanisms still leave much room to be optimized for the following reasons. First, in the new trend of cloud computing networks, datacenters are pushed to the edge of networks to reduce latency (they are called edge datacenters). Such datacenters are often deployed in geographically distributed buildings and collocated with offices in terms of sharing building infrastructure; such buildings are called geo-distributed mixed-use buildings (geo-MUBs). That scenario has not been well addressed in terms of energy sustainability requirements overall in the buildings; the requirements are imposed either by mandatory government orders or by LEED certification. Second, one critical issue of datacenters is water saving, which is rarely associated with energy efficiency, even though every kilowatt of energy consumption can reflect exactly an amount of water use in datacenters. Therefore, in this paper, we aim to find a solution for joint energy scheduling and water saving problem ($\mathbf{P_{JEW}}$) in a coordinated manner between MUBs. The solution is designed to schedule workloads by coupling edge datacenters collocated in buildings as well as to control energy and water usage to minimize the system cost caused by reducing loads. We advocate the model predictive control (MPC) to schedule the whole system in a time horizon. Multiple simulation scenarios are evaluated to show the efficiency of our proposed methods compared to conventional approaches. The results reveal that our mechanism outperforms the uncoordinated methods and achieves a nearly optimal solution.**

***Index Terms*—Demand Response, Mixed-Use Building, Geographically Distributed Datacenters.**

I. Introduction

A challenging issue when building smart cities with efficient and reliable energy systems is to optimize the energy demands of buildings; it is being addressed in the smart grids. According to [1], buildings exhaust for nearly 40 percent of the U.S. primary energy consumption and 70 percent of the electricity use. Even though existing solutions improve building energy efficiency via several methods, for the energy optimization for buildings, many problems still exist that need to be tackled both by businesses and in the literature. In particular, overlooking energy issues in buildings, prior works have omitted or not addressed well the important aspect: *the relationship between energy and water use in the colocation scenario*, in which multiple loads (e.g., datacenters [DCs], offices) are collocated in a building, in which they share facilities such as electric lines, heating, ventilation, and air conditioning (HVAC) systems [2]. Such a colocation scheme has received much attention in research for the following reasons. First, colocation of energy loads occurs in a building with a shared infrastructure, called a mixed-use-building (MUB) [3], in which the building operator needs efficient mechanisms to answer both energy and water demands of all colocation loads. Currently, datacenters already account for over 2% of all energy usage, and a majority of datacenters are located in MUBs. It is estimated that MUBs with datacenters take up about 4% of the total energy usage [3]. Importantly, as highly-distributed edge datacenters are becoming increasingly more pervasive to host latency-critical Internet of Things applications, MUBs with datacenters onsite will also experience a rapid expansion. Second, as presented in [4], datacenters are not only "hungry" for energy, but also "thirsty" for water to operate their systems, where millions of gallons of water are required for cooling and electricity production. Nevertheless, prior works on datacenters often focus separately on energy or water problems without considering a coupling scenario for those demands. Finally, many developers and owners are currently seeing MUBs as an opportunity for energy efficiency in relation to building efficiency and sustainability. Buildings are further leveraged to achieve green certifications (e.g., through the LEED program [5]). Especially, colocations of MUB architectures are suggested for dense metropolitan areas, where green programs are critical for cutting loads at peak demand times [6].

To find a solution for MUB architecture with datacenters, optimization mechanisms are not now being well addressed, as datacenter infrastructures have become smaller and more distributed. Because of the small size of infrastructure, multiple loads in MUBs can be easily collocated within a building and share building infrastructures. Indeed, with smaller infrastructures, each energy load in an MUB (whether datacenter or non-datacenter) may not shed sufficiently amount of reduction energy required by green programs, such as demand response (DR) programs and the LEED certificate. Furthermore, those loads cannot directly participate in such green programs because the grid can monitor only the building's power, not individual loads to apply traditional approaches, as in dedicated datacenters.

Last but not least, existing optimization models focus

Corresponding author: Dr. C.S. Hong (Email:cshong@khu.ac.kr).

This article has been accepted for publication in a future issue of this journal, but has not been fully edited. Content may change prior to final publication. Citation information: DOI 10.1109/TSG.2018.2880654, IEEE Transactions on Smart Grid

mainly on individual energy or water model in datacenters and buildings. While energy source can be clearly seen as a coupling aspect on those loads, the water source appears to be a hidden one with few concerns in MUBs. For example, prior works on buildings [2], [3] considered the energy optimization of all loads in the MUB including the HVAC system; but they did not exploit the relationship between energy and water in the MUB. The discussion in [7] mainly concerns the water issue in geo-distributed datacenters, whereas edge datacenters are now colocated with offices in shared building infrastructures. The more energy a building uses, the more water it needs to alleviate the building heat by operating the cooling system.

In this paper, we consider the problem of *joint energy and water saving in a geographically distributed mixed-use buildings* (geo-MUBs) scenario. We mainly target *a joint energy sustainability and water saving strategy* in terms of capturing workload distribution and energy and water use of all colocation loads in all buildings. In particular, the presence of edge datacenters spatially couples different buildings in different locations as a result of geographic load balancing capability. In addition, the concern with colocation office loads will be to give a dynamic and flexible control load in buildings overall. Using a joint energy sustainability and water saving strategy, we specifically involve a scheduling mechanism to operate the whole system in a time horizon. Furthermore, an energy capping is used to enable remarkable benefits for MUBs imposed either by mandatory government orders or by LEED certification [7]. Furthermore, we propose a distributed mechanism for MPC based on the dual decomposition framework [8] where the computation is executed in a distributed manner.

A summary of the major contributions of this paper follows:

- We formulate an optimization problem for scheduling multiple loads in geo-MUBs (called $\mathbf{P_{JEW}}$) to minimize the total cost incurred in the system while satisfying the energy sustainability constraint.
- We develop an offline distributed algorithm to solve $\mathbf{P_{JEW}}$ based on the dual decomposition framework, whereby we can schedule the energy load, water use and datacenter workloads in a time horizon, called JEWAS-OF (the offline algorithm for joint energy scheduling and water saving). Further, to address $\mathbf{P_{JEW}}$ with uncertainty workloads, we propose an online algorithm derived from JEWAS-OF, called JEWAS-ON.
- We conduct the performance of our method using a real trace of workloads in a time horizon. The simulation results show that our approach can achieve substantial cost saving for the whole system compared to current practices.

The rest of this paper is organized as follows. Section II summarizes some of the current approaches related to building energy management in the literature. In Section III, we introduce the system model and the problem formulation of the geo-MUB system. Section IV presents the design of MPC with certainty/uncertainty demand workloads. We perform the simulation to evaluate the system in Section V. Finally, we conclude the paper in Section VI.

II. Related work

Recently, several green programs have paid attention to particular buildings and datacenters, such as DR, LEED. Without considering the colocation scenario, non-datacenters in buildings can reduce the power consumption through global thermostat setpoint setback control, supply air temperature adjustment, pre-cooling, and use of a discharging energy storage device (e.g., battery) [9]–[11]. Focusing on the HVAC system in buildings has received much attention in business and research since HVAC consumes most power in buildings [11]–[13].

Unlike regular buildings, MUBs are a specific kind of buildings in which multiple loads coexist and share building infrastructures. Especially, the datacenter load is an important factor that creates several concerns for MUBs to optimize energy consumption. For conventional datacenters, many energy optimization approaches have been proposed and implemented in real systems by consolidation [14], scaling down CPU frequencies [15], dynamically turning on/off servers in owner-operated datacenters [16], [17] and performing load balancing of the workloads [18]. Because they own all the infrastructure from IT workloads, servers and network systems to the cooling system, dedicated datacenters have many control knobs to help reduce energy use [19]. Unfortunately, these methods are difficult to apply directly in MUBs since MUB loads are often too small to individually reduce energy for green programs. MUBs now need efficient and dynamic coordination approaches to control overall loads in a building as well as in remote buildings.

In the first study on the coordination approach in MUBs, the authors of [3] proposed a cost-effective method in DR via coordinated energy management. This work investigated the concept of MUBs and illustrated the effectiveness of coordinated energy management compared to individual load control. We continue and develop this approach with an incentive mechanism that distributes shedding energy reduction to each MUB tenant in order to minimize the total incurred cost [20]. Despite having achieved the minimum total cost compared to the state-of-the-art methods, these proposed mechanisms do not focus on coupling multiple loads in geo-MUBs, in which edge datacenters can be located in different buildings at different locations because of the geographical load balancing capability. An important aspect, water saving, which is non-trivially related to the energy usage in buildings, has not been addressed well. As a result of the colocation, a building operator has to supply efficiently the power demand as well as the water demand of all building loads, which has recently become a substantial issue [4], [21], [22]. The mutual relationship between energy and water makes the joint energy-controlling and water-saving problem more critical and significant when building operators are trying to achieve green building certifications (e.g., the LEED certificate).

III. System Modeling

We consider a typical geo-MUB scenario that includes I sites with different electrical utility service regions where

This article has been accepted for publication in a future issue of this journal, but has not been fully edited. Content may change prior to final publication. Citation information: DOI 10.1109/TSG.2018.2880654, IEEE Transactions on Smart Grid

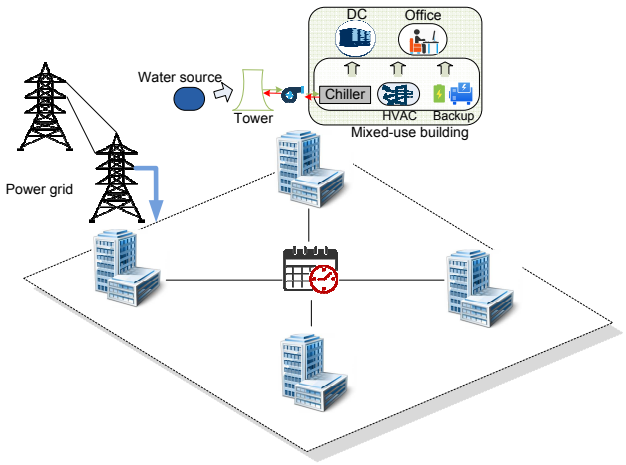

Fig. 1: The system model of geo-MUBs.

MUBs are located. Our proposed model is formulated to target overall joint energy sustainability and water saving in buildings during a time horizon T. At an MUB, the datacenter i is colocated with a set of non-datacenters (offices). All energy loads (i.e., from datacenters to non-datacenters) in a building are managed by the MUB operator and share the electricity, HVAC and the backup system (including a fuel generator and an energy storage). We consider the MUB energy usage is daily consumption by a *per-day energy cap constraint* (it will be explained later). Therefore, we schedule energy and water consumption of all loads in 24 hours such that all loads can satisfy an energy cap imposed by green programs in advance. The system model is depicted in Fig. 1.

A. Energy consumption for HVAC load in MUB

In this paper, we consider a share HVAC system in each MUB, including water pump, chiller and cooling tower. The thermal load in an MUB is refreshed via heat exchange from chiller water and supply air. We consider the amount of thermal load in building i as follows [23]:

$$H_i(t) = \left[T_i^{DC}(t) - T_i^{supDC}\right] r_i^{DC}(t) c_i + \left[T_i^{Of}(t) - T_i^{supOf}\right] r_i^{Of}(t) c_i, i = 1, 2, ..., I, \quad (1)$$

$$[T_i^{chw} - T^{supchw}] r_i^{chw}(t) c_i^w + [T_i^{cw} - T_i^{supcw}] r_i^{cw}(t) c_i^w \geq H_i(t), i = 1, 2, ..., I, \quad (2)$$

where $T_i^{Of}(t)$, $T_i^{DC}(t)$ denote the temperature in offices and in datacenters of MUB i at time t, respectively; T_i^{supDC} and T_i^{supOf} denote the supply temperature in datacenters and offices of MUB i, respectively; $r_i^{DC}(t)$ and $r_i^{Of}(t)$ denote the air flow rate in datacenters and offices and c_i denotes the heat capacity of air in MUB i; T_i^{chw}, T^{supchw}, T_i^{cw}, and T_i^{supcw} denote the return and the supply chilled water temperature, the return and the supply condensed water temperature, respectively; c_i^w denotes the water capacity. Those parameters are given in our model for the heating calculation.

At timeslot t, the building i needs to alleviate the amount of heat $H_i(t)$ by controlling the flow rate of the chiller water $r_i^{chw}(t)$ and condensed water $r_i^{cw}(t)$. Following [23], the amount of energy demand for HVAC is consist of the chiller water $e^{chw}(r_i^{cw}(t))$ the pump system $e^{pump}(r_i^{chw}(t))$ and the tower $e^{tow}(r_i^{cw}(t))$. These energy loads are calculated according to the flow rate of chiller water and condensed water [23]. Specifically, we present all the calculation and the constraints of the HVAC system as follows:

$$e_i^{hvac}(t) = e_i^{chw}(r_i^{cw}(t)) + e_i^{pump}(r_i^{chw}(t)) + e_i^{tow}(r_i^{cw}(t)), i = 1, 2, ..., I. \quad (3)$$

$$e_i^{chw}(r_i^{chw}(t)) = \alpha_0 + \alpha_1 r_i^{chw}(t) + \alpha_2 r_i^{chw}(t)^2 + \alpha_3 r_i^{chw}(t)^3, \quad (4)$$

$$e_i^{pump}(r_i^{chw}(t)) = \beta_0 + \beta_1 r_i^{chw}(t) + \beta_2 r_i^{chw}(t) + \beta_3 r_i^{chw}(t), \quad (5)$$

$$e_i^{tow}(r_i^{cw}(t)) = \gamma r_i^{cw}(t)^3, \quad (6)$$

with $\alpha_0, \alpha_1, \alpha_2, \alpha_3, \beta_0, \beta_1, \beta_2, \beta_3$ and γ are coefficients. From (1) to (6), these constraints illustrate how the building heat is refreshed and the relation between the building thermal load ($H_i(t)$) and the chilled and condensed water flow rates in building i.

According to ASHAE [13], the best guide for temperature setting of offices is from 18^{o}C to 27^{o}C and the maximum humidity is 60% for our simplified assumption under summer conditions.

B. Edge datacenters in MUBs

Traffic workloads and network constraints. Suppose that each MUB datacenter i consists of S_i servers, which are assumed to be homogeneous in this work. An MUB datacenter with heterogeneous servers can be viewed as multiple virtual datacenters, each having homogeneous servers. In general, each MUB datacenter deals with two types of workloads: *delay-sensitive workloads*, such as Internet services, and *tolerant-batch workloads*, such as indexing data, consolidation system. The response time of delay-sensitive workloads is strictly imposed (usually in milliseconds), while delay-tolerant workloads can be scheduled to run at any time as long as they can be finished. We formulate the constraints of workloads as follows.

For delay-sensitive workloads, the total incoming workloads $\Lambda(t)$ is driven to the main controller (called the geo-MUB controller), who receives the requests from users in a specific scheduling period T. We define a parameter $\lambda_i(t)$ as the amount of interactive workloads distributed to datacenter i at timeslot t, satisfying the following load balancing constraint:

$$\sum_{i=1}^{I} \lambda_i(t) = \Lambda(t), t = 0, ..., T-1. \quad (7)$$

For delay-tolerant workloads, let $b_i(t)$ and $\tilde{b}_i(t)$ denote the number of batch workloads requested and the number of batch workloads being served at datacenter i at timeslot t, respectively. In this work, following prior studies [24] and [2], we suppose that the delay-tolerant workloads are not migrated to other datacenters because of their expensive migration cost. Since this type is the deferrable workloads, the

This article has been accepted for publication in a future issue of this journal, but has not been fully edited. Content may change prior to final publication. Citation information: DOI 10.1109/TSG.2018.2880654, IEEE Transactions on Smart Grid

constraint to fulfill the demand of delay-tolerant workloads can be formulated as follows:

$$\sum_{t=0}^{T-1} b_i(t) = \sum_{t=0}^{T-1} \tilde{b}_i(t), i = 1, ..., I. \quad (8)$$

Energy consumption of MUBs. Inspired by the calculation in [25] and [26] that represents the power consumption depending on server utilization, we assume that all workloads driven to datacenter i will be evenly distributed to all active servers. Hence, the energy of MUB datacenter i at time t to serve the amount of demand workloads $d_i(t) := \lambda_i(t) + b_i(t)$ is as follows $s_i(t)\Big(p_{i,s} + p_{i,a}\frac{d_i(t)}{s_i(t)\mu_i}\Big) PUE_i$, where s_i is the number of active servers at slot t for serving demand workloads, $p_{i,s}$ and $p_{i,a}$ are the static and active powers of each server at MUB datacenter i, respectively, μ_i is a server's service rate measured in terms of the amount of workloads processed per unit time at datacenter i, $\frac{d_i(t)}{s_i(t)\mu_i}$ is the server utilization at time t and PUE_i is the power usage effectiveness of datacenter i, which is measured by IT plus non-IT power consumption divided by IT power consumption. Therefore, the total energy allocated for serving the demand workloads is calculated as follows:

$$e_i^{DC}(d_i(t)) = s_i(t)\Big(p_{i,s} + p_{i,a}\frac{d_i(t)}{s_i(t)\mu_i}\Big) PUE_i, \forall i \in \mathcal{I}. \quad (9)$$

The service-level agreement (SLA) constraint in MUB datacenters. Consider that MUB datacenter i at timeslot t is serving the demand workloads with $\tilde{b}_i(t) = 0$. Using the M/M/1 queue model, the constraint of datacenter i's delay-sensitive workloads is as follows:

$$\frac{1}{\mu_i - \frac{\lambda_i(t)}{s_i(t)}} \leq D_i, \quad (10)$$

where D_i is the SLA threshold at MUB datacenter i. The constraint corresponds to the maximum delay of the tolerant workloads at MUB datacenter i. This formulation of the SLA constraint is widely used as a measurement of **quality of services (QoS)** [2], [7], [17], [25]. When reducing the power consumption by switching off servers, the controller has to guarantee the SLA constraint (10). From this constraint, we can derive the threshold of the number of active servers in MUB datacenter i as follows:

$$s_i(t) \geq \frac{\lambda_i(t)}{\mu_i - 1/D_i} := \underline{s}_i(t). \quad (11)$$

Combining (9) and (11), the minimum power demand at MUB datacenter i is bounded as follows:

$$e_i^{DC}(d_i(t)) \geq \left(\underline{s}_i(t)p_{i,s} + \frac{p_{i,a}d_i(t)}{u_i}\right) PUE_i, i = 1, 2, ..., I \quad (12)$$

C. The backup system

We consider multiple factors of the backup system that include a fuel generator and an energy storage unit (e.g., a battery). In order to prevent a power outage disaster, having a backup system in place is required to provide buildings with temporary power during an emergency. We define $e_i^{b+}(t)$ and $e_i^{b-}(t)$ as the discharged and charged energy from the battery at time t, respectively. Let $L_i^b(t)$ be the level of the battery at time t. The dynamics of the storage unit are represented as follow:

$$\underline{L}_i^b \leq L_i^b(t) \leq \bar{L}_i^b, \quad (13)$$

$$L_i^b(t+1) = L_i^b(t) + e_i^{b+}(t) - e_i^{b-}(t), \quad (14)$$

$$L_i^b(T-1) \geq L_i^b(0), \quad (15)$$

$$|e_i^{b-}(t)| \leq \kappa, \quad (16)$$

$$e_i^{b+}(t), e_i^{b-}(t) \geq 0. \quad (17)$$

Constraint (13) indicates the limitation level of the battery in charging and discharging. Constraint (14) shows the dynamic level of the battery in our scheduling. And (15) states the balance in our system, where the battery should be recharged at the end of the schedule or at least, its power should be equal to the initial level $L_i^b(0)$. Finally, (16) reflects the time constraint of energy level in charging/discharging the battery, where for each timeslot, the battery can charge/discharge up to κ.

Furthermore, we consider the fuel backup generator in which we use $e_i^{bg}(t)$ to define the power supplied from the fuel generator at time t in building i. For ease of notations, we define $e_i(t) := e_i^{nonDC}(t) + e_i^{DC}(t) + e_i^{b-}(t) - e_i^{bg}(t) - e_i^{b+}(t)$, where $e_i^{nonDC}(t) := e_i^{hvac}(t) + e_i^{mis}(t)$, with $e_i^{mis}(t)$ is the energy of miscellaneous purposes of offices in building i at time t. This parameter ($e_i^{mis}(t)$) is given in our model (i.e., it means that the system needs to collect the value of every timeslot t).

In this work, miscellaneous loads are defined as any load that depends mainly on the occupant behaviors and can be gathered based on traditional methods [27], [28]. Due to the unimportant load, these loads are the given input parameters in our model in every timeslot. Even though the system does not need to predict those given parameters, the varying miscellaneous loads during T timeslots that capture the reality of the environment raise challenges for scheduling methods to adapt to the dynamic system. Therefore, the input miscellaneous loads are the considerable value in our work.

D. MUB water: on-site direct water usage

It is difficult to measure the water-usage statistic for datacenters in both research and practice. This issue seems more difficult in terms of colocation for the following reasons. First, all datacenters use energy, but not all use water. Among of those that use water, the amount of water use depends on the cooling system, which is equipped in datacenters or buildings for heat rejection. The more energy used, the more heat needs to be rejected. The amount of water usage in the cooling system reflects the amount of energy usage, but it is also affected significantly by the outside environment (e.g., temperature, humidity). Second, the quality of water usage cannot be easily equated; some datacenters use fresh water, "gray water" or even saltwater. Finally, in the shared scenario of colocation, water may be used for various purposes that do not reflect exactly the amount of water used by datacenters.

This article has been accepted for publication in a future issue of this journal, but has not been fully edited. Content may change prior to final publication. Citation information: DOI 10.1109/TSG.2018.2880654, IEEE Transactions on Smart Grid

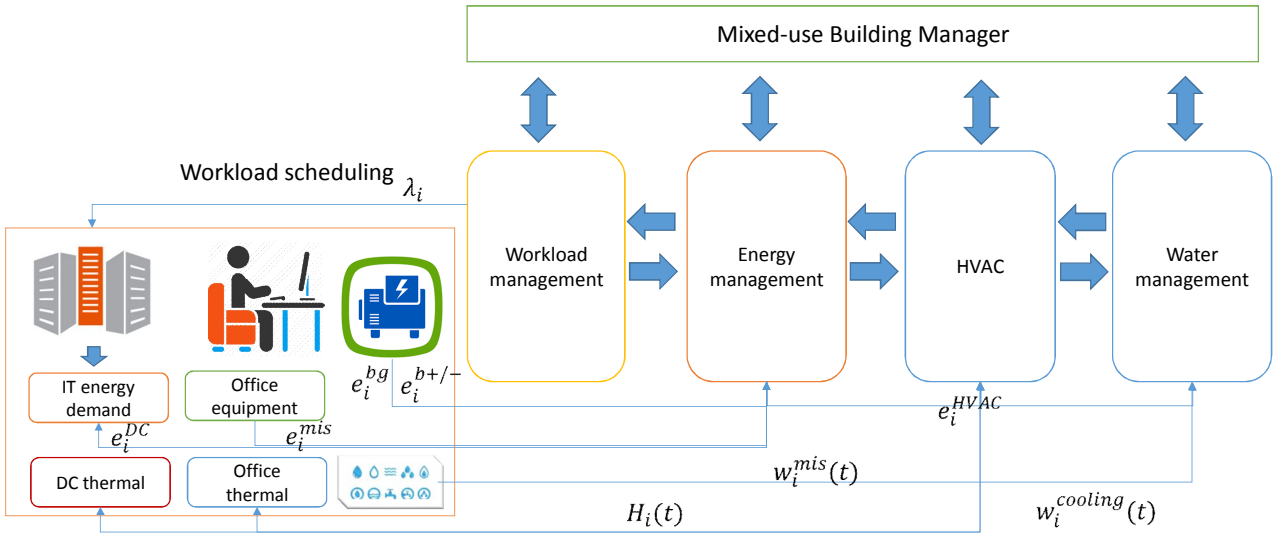

Fig. 2: The model of geo-MUBs management.

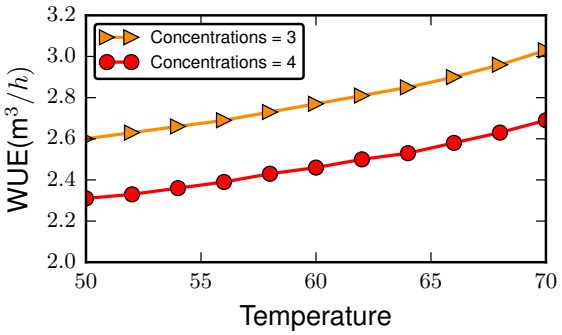

Fig. 3: The impact of wet bulb temperature on the direct WUE [29].

These difficulties have led to a few reports on water saving for datacenters and state-of-the-art buildings.

In general, our work assumes that a cooling system exists in every building and that it is shared for all loads. Hence, the on-site direct water consumption in a building is from cooling towers and miscellaneous purposes. Following [4], we use the coefficient parameter Water Use Effectiveness (WUE), which is considered the industry standard in measuring datacenter water use. In particular, WUE is a metric developed by The Green Grid to help data centers measure the ratio of total water consumption to IT energy usage. A higher WUE ratio implies a more intensive use of water in datacenters. The WUE of one building differs from that of others for multiple reasons, but mostly because of different cooling systems. Specifically, cooling towers are deployed in datacenters for heat rejection with two major factors that impact water consumption, namely, water quality [7] and water evaporation. Because our scenario occurs in a city, we assume that all the buildings have the same water quality. Another factor-affecting the cooling tower is water evaporation, which is highly determined by the outside wet bulb temperature. Based on an industry experiment [29], Fig. 3 shows the impact of outside wet bulb temperature on WUE. It illustrates clearly the increase of WUE when the outside wet bulb temperature increases (because the high-temperature results in a high loss of water though evaporation into the air).

Given a cooling system, we assume that building i can directly measure WUE in every timeslot t based on the calculation with the outside wet bulb condition [29]. We define the WUE function for each building as follows:

$$\text{WUE}_i(t) = \frac{c}{c-1}[6.10^{-5}(T_i^b(t))^3 - 0.01(T_i^b(t))^2 + 0.61T_i^b(t) - 10.40], \quad (18)$$

where c_i is the cycle of concentrations and $T_i^b(t)$ is the outside wet bulb temperature at building i.

To calculate the water usage in buildings, we define $\omega_i(t)$ as the amount of water usage at MUB i, where the water use in buildings is from i) the cooling system depending on the energy usage as well as the outside condition as presented in [4], and ii) the amount of water usage for miscellaneous purposes, such as irrigation and toilet flushing, etc. Consequently. we formulate the MUB water usage in MUB i as follows:

$$\omega_i(t) = e_i(t)\text{WUE}_i(t) + \omega_i^{mis}(t), \quad (19)$$

where ω_i^{mis} is the water usage for miscellaneous purposes. Similar to the miscellaneous energy load, the miscellaneous water usage ω_i^{mis} is given in our model. Consequently, (19) reflects the dependency of water usage on both energy consumption in a building and the outside temperature. Hence, MUB energy management needs to be temperature-aware, whereas the existing energy management systems tend to ignore water consumption that is obviously in relation to temperature.

This article has been accepted for publication in a future issue of this journal, but has not been fully edited. Content may change prior to final publication. Citation information: DOI 10.1109/TSG.2018.2880654, IEEE Transactions on Smart Grid

E. Operational costs

There are multiple factors in our joint optimization problem. We apply the weighted sum [30] to model the geo-MUB problem. With aforementioned notational conventions, we formulate the geo-MUB load management in terms of reducing the system cost as follows

$$\begin{aligned} C_i(t) =& P_i^{nonDC} e_i^{nonDC}(t) + P_i^{DC} e_i^{DC}(t) + P_i^{b+} e_i^{b+}(t) \\ &+ P_i^{b-} e_i^{b-}(t) + P_i^{\omega} \omega_i(t) + P_i^{bg} e_i^{bg}(t), \forall i = 1, ..., I. \end{aligned} \tag{20}$$

where P_i^{nonDC}, P_i^{DC}, P_i^{b+}, P_i^{b-}, P_i^{ω}, and P_i^{bg} are the weight factors that reflect the importance of non-datacenter load energy, datacenter energy, discharging and charging energy, water and the fuel backup system respectively in MUB i at time t. As represented in (20), the system cost in geo-MUBs is caused by the amount of energy and water use as well as how the backup system is handled.

Note that: the cost in (20) reflects a dynamic control in our model, in which we can scale the system as a green load balancing datacenters' points of view to a coordination of multiple load scenarios in MUBs by adjusting the weight parameter (the impact of the weighted parameters will be discussed concretely in the simulation section).

F. Mixed-Use Building management

With aforementioned formulations, we provide a flow model for geo-MUB management in Fig. 2. We design the system with multiple related components, each of which has a specific responsibility, while they communicate through the Internet or a private network.

Mixed-use building manager module. At the top of the model, we implement a mixed-use building manager module as the main controller that can carry out the optimization algorithm to answer the queries from lower components, such as the workload management component, the energy management component, the HVAC component and the water management component. These management components are implemented in all MUBs. Controlling information can go through the northbound interface to communicate between the controller and MUBs. The controller receives information about the workload arrival rate (from the workload component), energy demand from office equipment, the energy level of the battery (from the energy management component), the temperature, and humidity in offices (from the HVAC component) and the water condition (from the water management component) in the buildings. By executing the optimization algorithm, the mixed-use building manager will answer how many workloads can be scheduled at datacenter i, the amount of energy needed to handle the IT loads, HVAC and miscellaneous loads, and the amount of water usage at each MUB in every timeslot.

Workload management module. This scheduling workload module manages the workloads in our system, including the delay sensitive workloads, $\{\lambda_i(t)\}$, and batch workloads, $\{b_i(t)\}$. Based on the arrival rate workloads planned by the MUB manager, this component will operate workloads at the datacenter, such as operating a number of active servers, and scheduling and executing workloads.

Energy management module. This module is responsible for managing the energy demand from datacenter operation, $\{e_i^{DC}(t)\}$, office equipment, $\{e_i^{mis}(t)\}$, HVAC system, $\{e_i^{hvac}(t)\}$ and the backup system, $\{e_i^{bg}(t), e_i^{b+/-}(t)\}$.

HVAC module. In order to handle the HVAC system, this module is responsible for collecting the information of temperatures in datacenters, $\{T_i^{DC}(t)\}$, offices, $\{T_i^{Of}(t)\}$, setting temperatures, $\{T_i^{supDC}, T_i^{supOf}\}$, the air flow rates, $\{r_i^{cw}(t), r_i^{chw}(t)\}$, to control the heat in the buildings.

Water management module. This module is responsible for managing the water usage in a building, including the amount of water usage for HVAC system $w_i^{hvac}(t) := e_i(t)\text{WUB}_i(t)$ and miscellaneous purposes $\{w_i^{mis}(t)\}$.

All management components in our model use the southbound interface to communicate in operation. Even though each component is responsible for a different task, they need to communicate in order to handle the shared infrastructure of the geo-MUB scenario. For example, to handle an amount of workload, the workload component needs to operate $s_i(t)$ active servers, which require an amount of energy supplied by the energy management component. Furthermore, this number of active servers results in increasing/decreasing the heat in datacenters; therefore the HVAC component is asked to adjust its air flow rates. To simplify our system, each model can be considered a black box that communicates to others through APIs. The execution strategy of each module operates transparently in relation to others.

G. Problem formulation and challenges

With all aforementioned constraints, we take into account a scheduling scheme in which the controller makes a decision for energy consumption and water usage in geo-MUBs during period T for cost saving. The problem is formulated as follows:

$$\mathbf{P_{JEW}}: \min \quad \sum_{t=0}^{T-1} \sum_{i=1}^{I} C_i(t) \tag{21}$$

s.t. HVAC constraints (1) - (6),

$$\sum_{t=0}^{T-1} \sum_{i=1}^{I} e_i(t) + e_i^{bg}(t) + e_i^{b}(t) \leq Q, \tag{22}$$

$$\sum\nolimits_{i=1}^{I} \lambda_i(t) = \Lambda(t), t = 0, ..., T-1, \tag{23}$$

$$\sum\nolimits_{t=0}^{T-1} b_i(t) = \sum\nolimits_{t=0}^{T-1} \tilde{b}_i(t), \tag{24}$$

$$e_i^{DC}(d_i(t)) = s_i(t)\Big(p_{i,s} + p_{i,a}\frac{d_i(t)}{s_i(t)\mu_i}\Big) PUE_i, \tag{25}$$

$$s_i(t) \geq \frac{\lambda_i(t)}{\mu_i - 1/D_i} := \underline{s}_i(t), \tag{26}$$

$$e_i^{DC}(d_i(t)) \geq \left(\underline{s}_i(t) p_{i,s} + \frac{p_{i,a} d_i(t)}{u_i}\right) PUE_i, \tag{27}$$

$$\underline{L}_i^b \leq L_i^b(t) \leq \bar{L}_i^b, \tag{28}$$

This article has been accepted for publication in a future issue of this journal, but has not been fully edited. Content may change prior to final publication. Citation information: DOI 10.1109/TSG.2018.2880654, IEEE Transactions on Smart Grid

Algorithm 1 JEWAS-OF: Distributed algorithm for $\mathbf{P_{JEW}}$

Initialization: Set ϵ_1, ϵ_2 and input parameter $\boldsymbol{s}$;
At each timeslot $\tau, \tau = t, ..., t+T$;
Initialize $k = 0$, $\upsilon^{(0)}, \phi^{(0)}$;
repeat
  $k \leftarrow k+1$;
  Each operator i receives $\upsilon^{(k)}$, and $\phi^{(k)}$;
  Compute $x_i^{(k)}$ by solving **P2**;
  Send $x_i^{(k)}$ to the controller of building i;
  Operator updates $\upsilon^{(k+1)}$, and $\phi^{(k+1)}$ by (40) and (41);
until $\|\upsilon^{(k)} - \upsilon^{(k-1)}\|_2 < \epsilon_1$ and $\|\phi^{(k)} - \phi^{(k-1)}\|_2 < \epsilon_2$;

$$L_i^b(t+1) = L_i^b(t) + e_i^{b+}(t) - e_i^{b-}(t), \quad (29)$$
$$L_i^b(T-1) \geq L_i^b(0), \quad (30)$$
$$|e_i^{b-}(t)| \leq \kappa, \quad (31)$$
$$\omega_i(t) = e_i(t)\text{WUE}_i(t) + \omega_i^{mis}(t), \quad (32)$$
$$e_i^{b+}(t), e_i^{b-}(t) \geq 0, \quad (33)$$
$$i = 1, ..., I,$$

where Q in (22) is the limitation of the energy consumption allocated for geo-MUBs during period T. The total energy consumption constraint can be interpreted as an "energy cap", which is used to formulate a highly-desired sustainability issue in MUBs (e.g., due to government orders, the LEED certification, etc.). With this kind of sustainability issue, *the energy capping is represented by the amount of per-day energy cap [24] through converting allocating the monthly energy cap into a daily cap*. However, this inequality constraint (22) can be relaxed to the equality constraint because every curtailing strategy always decreases the performance of MUB loads or increases the system cost created by the backup system.

In $\mathbf{P_{JEW}}$, we aim to pursue an online management during time horizon T for energy, water and workloads in a coupling scenario of different buildings in different locations because of the geographic load balancing capacity. The complexity of $\mathbf{P_{JEW}}$ increases exponentially when T is increased, and this is a critical challenge for every powerful solver.

IV. MPC SCHEDULING PROBLEM

In Section III, we account for optimizing the total operational cost during T timeslots. It implies that in the finite horizon, the operational cost must be minimized, subject to IT operational constraints (i.e., the constraints of demand workloads), thermal settings, as well as the limitation of energy usage constraint. We consider all sources of randomness as the state vector $s(t) := \{\Lambda(t), b_i(t), e_i^{mis}(t), T_i^{DC}(t), T_i^{Of}(t), \omega_i^{mis}(t), WUE_i(t)\}$ and also denote all the optimization variables as the vector $x_i(t) := \{\lambda_i(t), e_i(t), \tilde{b}_i(t), e_i^{bg}(t), e_i^{b+/-}(t)\}, \forall i \in \mathcal{I}$. For ease of notations, the cost function of each building i at timeslot t is re-written as follows: $g_i(x_i(t)) := C_i(t)$.

Invoking the main concept of the MPC method, we relax $\mathbf{P_{JEW}}$ to solve the deterministic problem over a planning horizon from current time t to $t+T$. Even though MPC is heuristic, it has some benefits, such as the simplification of complexity and more practical implementation than the dynamic programming method, where the computational complexity of the dynamic programming algorithm increases exponentially with the dimensionality of the state [31]. The main advantage of MPC is the iteration-based mechanism with a finite-horizon optimization of a scheduling model. At time t, it uses the current plan to sample, and it optimizes a control strategy for a relative time horizon $[t, t+T]$. Relying on iterative, finite-horizon optimization, MPC can simplify the complexity of calculation for solving complex problems, when the number of variables exponentially increases depending on the number of timeslots. It can be seen as a proper choice for solving $\mathbf{P_{JEW}}$; even though MPC in fact cannot guarantee an optimal result for the current timeslot, it does take future timeslots into account.

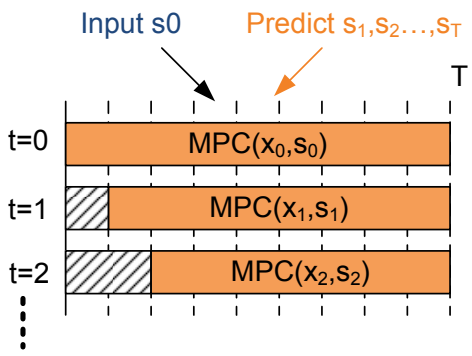

Fig. 4: The iteration-based mechanism of MPC.

To tackle the online problem $\mathbf{P_{JEW}}$, we execute iteratively the MPC scheduling until the system reaches the end timeslot, as illustrated in Fig. 4.

At each timeslot t, the controller creates a schedule for $\boldsymbol{x}$ from the input parameter $s(t)$ and predicting parameters $s(t+1), s(t+2), ..., s(t+T)$. Hence, $\mathbf{P_{JEW}}$ can be reformulated following MPC-based scheduling as follows:

$$\min \quad \sum_{\tau=t}^{T}\sum_{i=1}^{I} g_i(x_i(\tau)) \quad (34a)$$
$$\text{s.t} \quad \text{HVAC constraints (1) - (6)}, \quad (34b)$$
$$\sum_{\tau=t}^{T}\sum_{i=1}^{I} e_i(\tau) = Q(t), \quad (34c)$$
$$(23) - (33),$$

where $g_i(x_i(\tau)) := C_i(t)$, and the inequality constraint (22) can be relaxed to the equality constraint (34c) because every curtailing strategy always decreases the performance MUB loads or increases the system cost created by the backup system.

The limitation of energy usage is updated in every timeslot:

$$Q(t) = Q - \sum_{\tau=0}^{t}\sum_{i=1}^{I} e_i(\tau). \quad (35)$$

We assume all predicted parameters $s(t+1), s(t+2), ..., s(t+T)$ can be achieved exactly based on some machine learn-

This article has been accepted for publication in a future issue of this journal, but has not been fully edited. Content may change prior to final publication. Citation information: DOI 10.1109/TSG.2018.2880654, IEEE Transactions on Smart Grid

ing techniques [32], [33]. We focus mainly on designing a scheduling mechanism in a time horizon for the geo-MUB system that can minimize the operational cost while coupling multiple loads in geo-MUBs.

To solve $\mathbf{P_{JEW}}$, we advocate the dual decomposition framework, which can solve this problem in a distributed manner.

A. Dual decomposition algorithm for $\mathbf{P_{JEW}}$

We start with the case where the controller has complete knowledge about the demand workloads; thus we consider it as the offline case and name the proposed algorithm the joint energy and water saving in geo-MUBs (JEWAS-OF). We can derive the partial Lagrangian function of the $\mathbf{P_{JEW}}$ problem as follows

$$L(x_i(\tau)) = \sum_{\tau=t}^{T}\sum_{i=1}^{I} g_i(x_i(\tau)) + \sum_{\tau=t}^{T} \upsilon_\tau \left(\sum_{i=1}^{I} \lambda_i(\tau) - \Lambda(\tau) \right) + \phi \left(\sum_{\tau=t}^{T}\sum_{i=1}^{I} e_i(\tau) - Q(t) \right), \tag{36}$$

where υ and ϕ are dual variables.

We apply the dual decomposition algorithm to solve $\mathbf{P_{JEW}}$, handling the computation in a distributed manner. All steps of Alg. 1 are presented as follows:

At iteration $k+1$:

x-update:

$$\mathbf{P1}: \min \quad \sum_{\tau=t}^{T}\sum_{i=1}^{I} g_i(x_i(\tau)) + \sum_{\tau=t}^{T}\sum_{i=1}^{I} (\upsilon_\tau)^{(k)} \lambda_i(\tau) + \phi^{(k)} \sum_{\tau=t}^{T}\sum_{i=1}^{I} e_i(\tau) \tag{37}$$

$$\text{s.t} \quad \text{HVAC constraints (1) - (6), (23) - (33),} \tag{38}$$

The sub-problem **P1** can be decomposed to be executed at I sites. Each building i performs a schedule to minimize the operational cost, depending on the amount energy to process demand workloads, the HVAC system and the backup system's status (i.e., the level of the storage unit) by solving problem **P2** as follows:

$$\mathbf{P2}: \min \quad \sum_{\tau=t}^{T} g_i(x_i(\tau)) + \sum_{\tau=t}^{T} (\upsilon_\tau)^{(k)} \lambda_i(\tau) + \phi^{(k)} \sum_{\tau=t}^{T} e_i(\tau) \tag{39a}$$

$$s.t \quad \text{HVAC constraints(1) - (6), (23) - (33).} \tag{39b}$$

Dual update:

$$\upsilon_\tau^{(k+1)} := \upsilon_\tau^{(k)} + \delta \left(\sum\nolimits_{i=1}^{I} (\lambda_i(\tau))^{(k+1)} - \Lambda(\tau) \right), \tag{40}$$

$$\phi^{(k+1)} := \phi^{(k)} + \delta \sum\nolimits_{\tau=t}^{T} \sum\nolimits_{i=1}^{I} (e_i(\tau))^{(k+1)}. \tag{41}$$

where δ is the step size [8] to update υ and ϕ.

Algorithm 2 JEWAS-ON: Online algorithm for geo-MUBs

1: **Initialization:** Set ϵ_1, ϵ_2 and input parameter $\boldsymbol{s}$;
2: At each timeslot $\tau, \tau = t, ..., t+T$;
3: Set $k = 0$, $\upsilon^{(0)}, \phi^{(0)}$;
4: Predict the sensitive workloads by (42);
5: Apply Alg. 1 with the predicted workloads $\hat{\Lambda}$;
6: Go to Step 2;

From this distributed algorithm, each building i receives information about other buildings via the control variables υ and ϕ. Then, each building can schedule its energy usage, and water usage, delay-tolerant workloads by solving **P2**.

B. Online scheduling with uncertainty

Next, we present the online scheduling algorithm with uncertainty demand workloads (called JEWAS-ON). We adapt JEWAS-OF to a setting in which future demand workloads are predicted on the basic of the current observation. As shown in the constraint (10), the number of workloads is related to the number of active servers in the system. Further, switching on/off severs frequently may increase the wear-and-tear cost. Therefore, to control flexibly and smoothly the number of active servers in datacenters, we propose a prediction mechanism to keep track of the peak workloads in the system at each timeslot t. Intuitively, the demand sensitive workloads in the next timeslot are predicted based on the ceiling function, which rounds up the peak workloads according to the average workloads in the history and the current workloads at timeslot t. The ceiling function is represented as follows:

$$\hat{\Lambda}(t+1) = \max \left(\frac{1}{t} \sum_{\tau=0}^{t} \hat{\Lambda}(\tau) + \xi^s, \hat{\Lambda}(t) \right), \tag{42}$$

where ξ^s represents the system disturbance of the delay-sensitive workloads. We present all steps of the online scheduling algorithm in JEWAS-ON, where for every timeslot τ, the input of workloads is calculated by (42).

V. Numerical Results

A. Settings

We consider a geo-MUB system with five buildings ($I = 5$) and the energy cap of all MUBs is set to 50 megawatts during 24 timeslots. For MUB datacenters, each tenant has a maximum of $S_i = 3000$ servers, and one server has an idle power $p_{i,s} = 200$ W and a peak power $p_{i,a} = 400$ W. The average PUE is set to 1.5, which is typical for datacenters [34], that is whenever a tenant consumes 1 KWh energy, the corresponding energy consumption at the geo-MUB level is 1.5 KWh. Following the assumption in Section III, all servers are homogeneous, with a service rate μ_i that is set from 2 to 4 (i.e., 2 to 4 units of workloads per second). The delay threshold D_i is set to 1 second, i.e., the maximum delay-sensitive of the service is 1 second.

The effectiveness of our method depends directly on the flexible weight set $\boldsymbol{P}$. Drawing on the current literature, we characterize our work with three weight sets to set the system

This article has been accepted for publication in a future issue of this journal, but has not been fully edited. Content may change prior to final publication. Citation information: DOI 10.1109/TSG.2018.2880654, IEEE Transactions on Smart Grid

in accordance with a green load balancing datacenter point of view or according to a geo-distributed MUB model as follows:

1) Weight set 1: By using this setting, our model can be set as a traditional green load balancing geo-distributed datacenter model, in which the HVAC (the non-datacenter load) and water factors are not considered. Consequently, the workloads are scheduled to satisfy all datacenter constraints in $\mathbf{P_{JEW}}$, and only the datacenters' energy usage and the backup system are minimized.
2) Weight set 2: With this weight set, the system can be set to coordinate datacenter loads and others in the MUBs without regarding the water saving aspect. Such a setting reflects a traditional MUB model in the literature. The workloads are scheduled to minimize not only the energy cost of datacenter loads but also the non-datacenter loads. The water saving aspect is not considered in this setting. As in weight set 1, the backup system is a necessary aspect to shed reduction energy by following requirements. Therefore, workloads are scheduled to datacenter loads without an outside temperature awareness.
3) Weight set 3: All aspects are combined in this setting. Here, the workloads are scheduled to minimize not only the energy consumption but also the water usage in MUBs. We use this weight set in our simulation to demonstrate the efficiency of our model.

In all the weight sets, the backup generator is considered as the worst case in terms of highest cost. Hence, we set the weight factor of the backup generator (P_i^{bg}) in a range from 0.3 to 0.48, while the weight of water use (P_i^b) is set in a range from 0.01 to 0.05. With this setting, the backup system is only executed at each building to compensate for the amount of exceeded energy consumption in order to satisfy the requirement of DR. For the WUE setting, we use the values from [29]. To reflect the geographical distributed scenario in our model, we scale WUE differently from 1.2 to 2. We also set randomly the amount of water for the miscellaneous purposes of a building from 200 to 1000 liters/timeslot, which is referred from [35].

We set the amount of energy consumption $e_i^{nonDC}(t)$ for HVAC systems in geo-MUBs from 100 KW to 300 KW, following the settings of the HVAC system in [13] for buildings in the summer condition. For edge datacenters, we simulate with the real workload data from Facebook [36] that is normalized so as to be adapted to our setting model. Because of the lack of access to the real data of the delay-tolerant workloads in datacenters, we randomly set the request workloads, which are presented in the given parameter arrival rates $b(t)$.

For the storage unit, we set the initial level to be full (i.e., $L_0^b(t) = \bar{L}_i^b$) and the empty level is set at 0 (i.e., $\underline{L}_i^b = 0$), which can be mapped to any minimum threshold as the real case in practice. The threshold of charging/discharging κ in our model is set at 200 KWh.

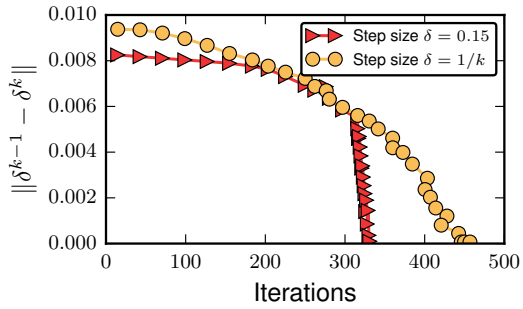

(a) The convergence with various step size values.

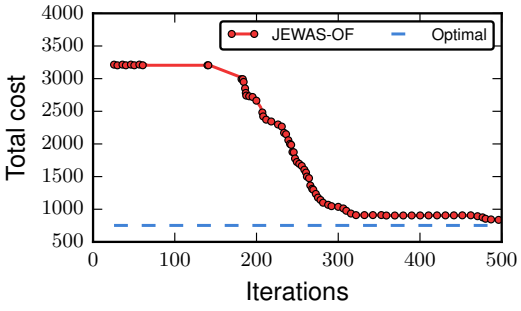

(b) The system operational cost.

Fig. 5: Convergence evaluation.

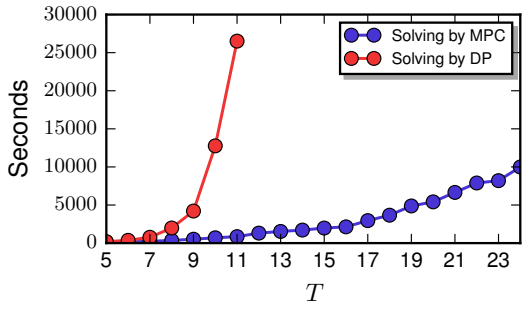

(a) Evaluation of execution time.

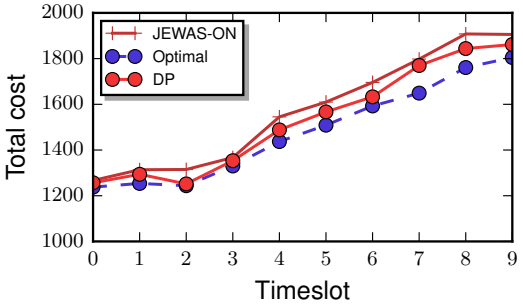

(b) Evaluation of the optimal gap.

Fig. 6: Optimality evaluation.

B. Results

1) Convergence: We evaluate the convergence of the total cost with different values of the step size δ. Fig. 5a shows the impact of the step size parameter on our algorithm. Using the dual decomposition method with the step size $1/k$, we achieve the fast convergence within 350 iterations. To further demonstrate the convergence of JEWAS-OF, we show the gap

This article has been accepted for publication in a future issue of this journal, but has not been fully edited. Content may change prior to final publication. Citation information: DOI 10.1109/TSG.2018.2880654, IEEE Transactions on Smart Grid

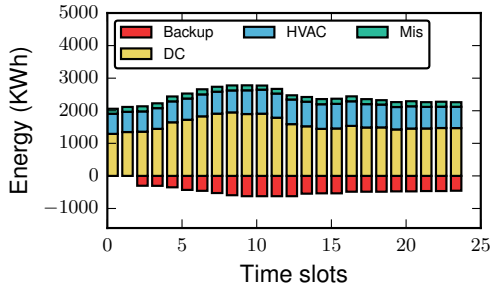

(a) Energy consumption.

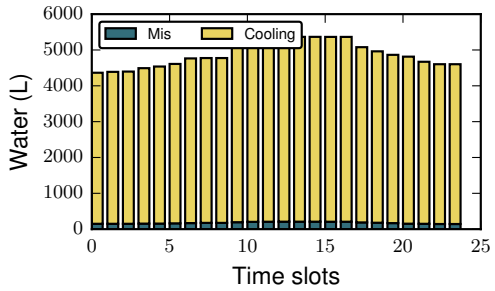

(b) Water usage.

Fig. 7: Evaluation of the weight set 1.

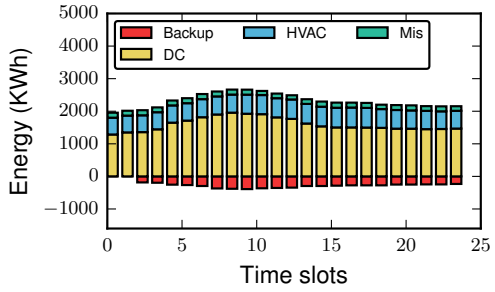

(a) Energy consumption.

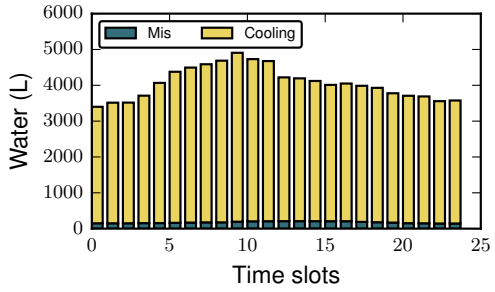

(b) Water usage.

Fig. 8: Evaluation of the weight set 2.

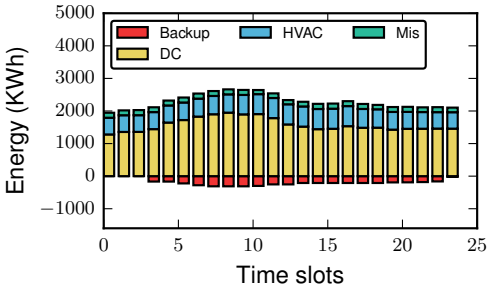

(a) Energy consumption.

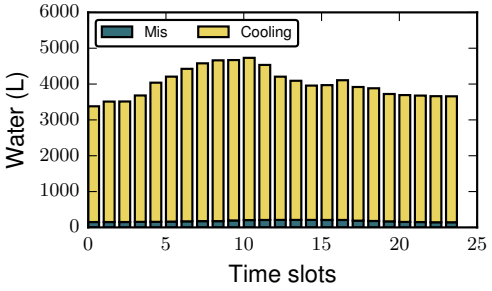

(b) Water usage.

Fig. 9: Evaluation of the weight set 3.

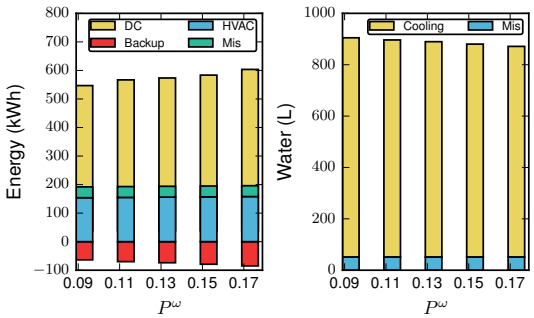

Fig. 10: Impact of the water weight parameter.

between JEWAS-OF and the optimal result in Fig. 5b.

2) Optimality: Furthermore, we evaluate the gap between our proposed mechanism and other benchmarks, including the DP approach and the optimal offline algorithm (i.e., given a complete offline information). Due to the high complexity of $\mathbf{P_{JEW}}$ with a large T, we set $T = 10$ for other benchmarks. In the case of DP, we apply the DP algorithm based on the recursive principle of the Bell-equation [31] with the initial point $J(\mathbf{x}(0))$. In particular, suppose $J^*(\mathbf{x}^*(T-1))$ to be the optimal result of $\mathbf{P_{JEW}}$ at timeslot $T-1$; then, $\mathbf{P_{JEW}}$ is equivalent to

$$L^*(\mathbf{x}^*(T-1)) + \min \quad \sum_{t=0}^{T-2} \sum_{i=1}^{I} g_i(x_i(t))\} \tag{43}$$

$$s.t. \quad (22) - (33) \tag{44}$$

In order to implement the evaluation, we use a Python simulation environment with a processor Intel Core i5 4300U

This article has been accepted for publication in a future issue of this journal, but has not been fully edited. Content may change prior to final publication. Citation information: DOI 10.1109/TSG.2018.2880654, IEEE Transactions on Smart Grid

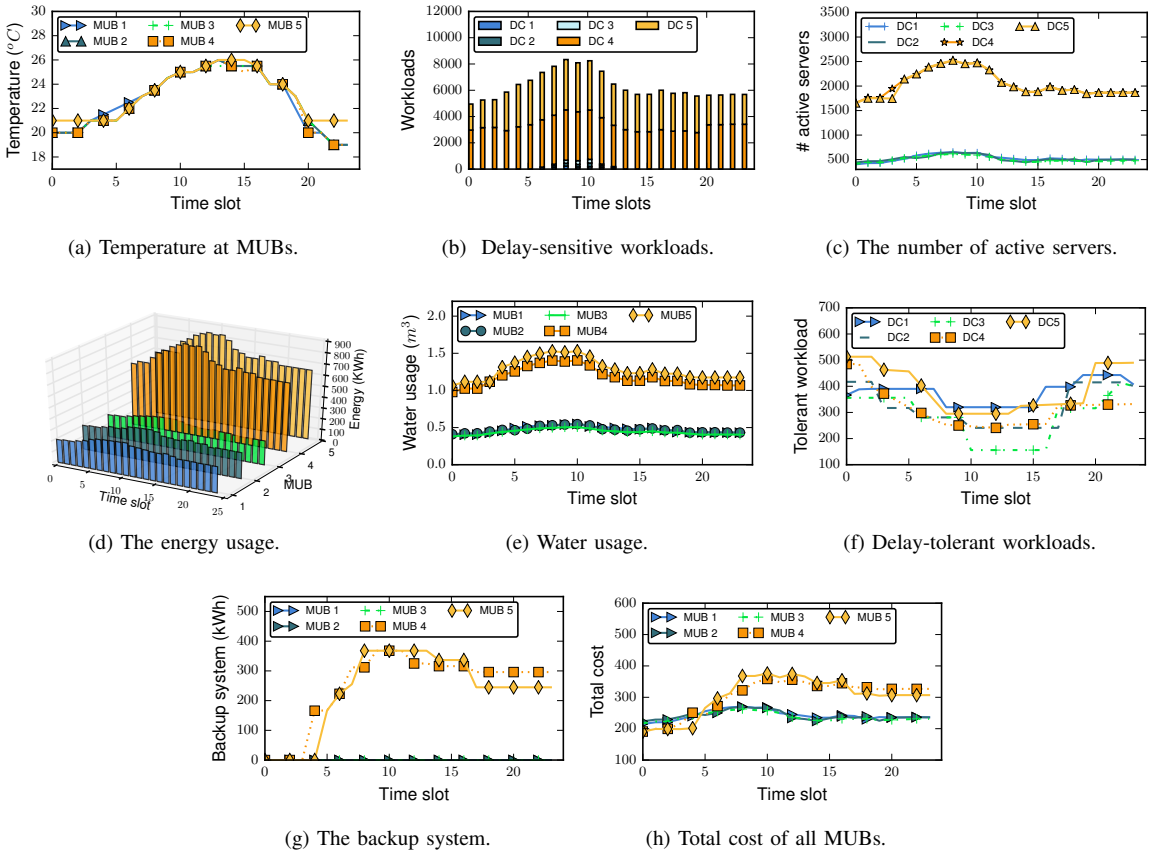

(a) Temperature at MUBs. (b) Delay-sensitive workloads. (c) The number of active servers.

(d) The energy usage. (e) Water usage. (f) Delay-tolerant workloads.

(g) The backup system. (h) Total cost of all MUBs.

Fig. 11: Scheduling multiple aspects in overall buildings.

Set	P_i^{nonDC}	P_i^{DC}	$P_i^{b+/-}$	P_i^{ω}	P_i^{bg}
1	[0.05-0.07]	[0.2-0.3]	[0.015-0.02]	[0.001-0.002]	[0.1-0.15]
2	[0.4-0.5]	[0.25-0.3]	[0.015-0.02]	[0.001-0.002]	[0.1-0.15]
3	[0.35-0.4]	[0.25-0.3]	[0.07-0.09]	[0.07-0.17]	[0.1-0.15]

TABLE I: Weight sets.

CPU @ dual 250 GHz to make a comparison between DP and MPC when scaling T, as shown in Fig. 6a. As a small $T < 7$, DP can converge very fast, but the convergence duration increases exponentially according to T. Fig. 6a also illustrates the applicability of MPC in our model with a diurnal setting $T = 24$. Though DP gives a better gap compared to the optimal offline result and JEWAS-ON, as illustrated in Fig. 6b, DP cannot be applied in the complex geo-MUB model with a diurnal consideration.

3) Effect of weight parameters: In agreement with the aforementioned setting, we conduct our evaluation on three given weight sets. We divide the setting of weight parameters into these sets corresponding to specific cases that can align control aspects with different priorities. For the detail, we provide all the weight settings in Table I.

- Weight set 1: In this weight set, we choose the low values for the weigh parameters of HVAC and water systems so that the system cost comprised mainly by the energy cost and the backup system. Without considering HVAC and water aspects, the workloads are scheduled in order to mainly reduce datacenter energy cost and the backup system. The result of this weight set is depicted in Fig. 7, where the workloads are scheduled to minimize only the datacenter energy loads. The inefficiency of this setting is revealed in Fig. 7a and Fig. 7b, with the very high shed energy of the backup system as well as the high water usages during 24 timeslots.
- Weight set 2: Using this setting, our system can be seen as a traditional MUB system [3], in which the water aspect is neglected by a very low weight value. Datacenters, HVAC and the backup system participate in the reduction energy issue. Unlike weight set 1, the participant of the HVAC results in the reducing energy of the backup system up to 39.6% compared to the result of weight set 1. The total energy consumption in MUBs is also reduced so that the water usage is lower than the outcome of weight set 1. All the results of this setting are presented in Fig. 8.
- Weight set 3: Using this weight setting, all aspects including HVAC, datacenters, backup system and water, are participated to minimize the system cost. To illustrate the result of this setting, we present the outcome in Fig. 9. The energy consumption of our system in 24 timeslots is reduced by 19% compared to the result of weight set 1. In addition, the water usage in this setting can be reduced up to 37% compared to the water usage in weight set 1. In addition, the amount of energy from the backup system

This article has been accepted for publication in a future issue of this journal, but has not been fully edited. Content may change prior to final publication. Citation information: DOI 10.1109/TSG.2018.2880654, IEEE Transactions on Smart Grid

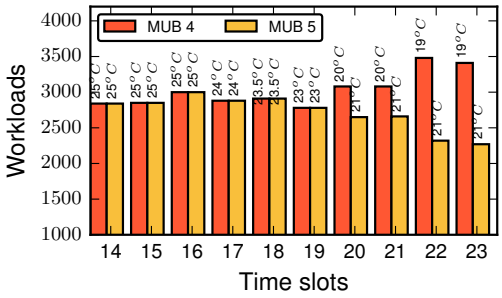

(a) Workload distribution in MUB 4 and MUB 5.

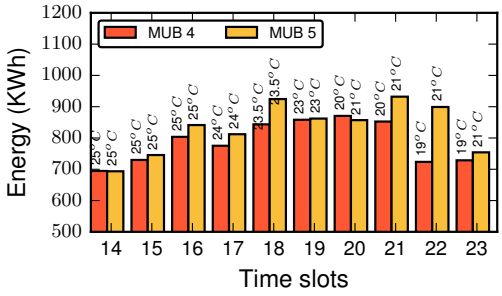

(b) Energy consumption in MUB 4 and MUB 5.

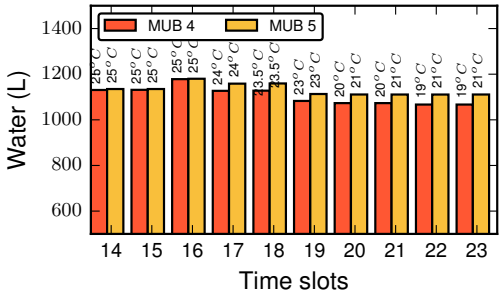

(c) Water usage in MUB 4 and MUB 5.

Fig. 12: The impact of temperatures.

is lower then the results of the prior weight sets.

In order to illustrate the efficiency of our designed method, we use weight set 3 for further evaluations in this work since it can include multiple aspects to control the system.

To further illustrate the impact of weight settings to control the energy and water loads in our model, we select MUB 5, which has the highest energy consumption and water usage among all the buildings. We then demonstrate the change of loads in the building at the peak workload period (e.g., the 9$^{\text{th}}$ timeslot) by varying the weight setting value P_i^{ω}, as shown in Fig. 10. When the weight setting value P_i^{ω} increases, the amount of water decreases, but the system needs to shed more energy from the backup system.

4) Effect of JEWAS-OF in geo-MUBs: Without uncertainty, we assume that the system can collect exactly the input information (such as workloads in a time horizon). Hence, we use the history of workloads to evaluate our proposed method. The snapshot of the schedule in all buildings during 24 timeslots is shown in Fig. 11. As the first measurement, we show the temperature changes of offices in all MUBs in Fig. 11a. We then demonstrate the dynamic of controlling workloads of our mechanism in Fig. 11b, which plots the delay-sensitive workload distribution in datacenters. This result is explained by our settings, where the service rates of servers in MUB 4 and MUB 5 are set to be higher than others. Thus, the delay-sensitive workloads achieved at these datacenters are dominant. However, at timeslots 19 to 23, the workloads are driven higher in MUB 4 than in MUB 5 because of its lower temperature. Also, due to this workload distribution, the number of active servers in these datacenters is greater than in MUBs 1, 2, and 3, as shown in Fig. 11c. In order to show the energy consumption of all loads, the snapshot during 24 timeslots is captured in Fig. 11d. Similar to the energy usage, the amount water usage of all MUBs is shown in Fig. 11e, where MUB 4 and 5 consume more water compared to MUBs 1, 2 and 3 in almost timeslots. Furthermore, the efficiency of our model is illustrated in Fig. 11f with the delay-tolerant workloads. This illustrates the dynamic control of our model, which is able to plan the execution of the delay-tolerant workloads at low-cost timeslots. We next evaluate the performance of the backup system. Fig. 11g shows the dynamic energy control of the backup system to ensure an energy capping requirement. With high energy demand, MUB 4 and MUB 5 need to supply more energy from the backup system to accommodate their loads' constraints. Finally, we show the total cost incurred in each MUB during all scheduling timeslots in Fig. 11h. The changes of system costs during 24 timeslots corresponding to workload scheduling, and the energy and water usage of each MUB are reflected in this figure.

5) Effect of outside temperatures in geo-MUBs: As shown in the system model, a change in outside temperature $T_i^b(t)$ will affect our control decisions, since it is involved in the water usage calculation. In particular, a higher outside temperature causes higher water usage in a building as well as affecting the system cost. As the input of our model, we plot the change of outside temperatures in MUBs during 10 timeslots, as shown in Fig. 12. From timeslot 14 to timeslot 19, the sensitive workload distribution at MUB 4 and MUB5 is similar, but it varies after that. More workloads are navigated to MUB 4 corresponding to its lower temperature, as shown in Fig. 12a. In contrast, MUB 5 consumes higher energy compared to MUB 4, even though the workloads are scheduled less than MUB 4. Similar to energy, the water usage at MUBs also reflects sensitively the temperature change as shown in Fig. 12c.

6) Effect of JEWAS-ON on geo-MUBs: To evaluate the online mechanism of our work, we create a simulation within 24 timeslots. The result is compared to the real workloads and optimal values of energy and water usage in MUBs, as shown in Fig. 13. In particular, Fig. 13b and Fig. 13c illustrate the small gap between the prediction result and the optimal value. These outcomes during 24 timeslots show that the MPC mechanism can produce a nearly optimal result.

This article has been accepted for publication in a future issue of this journal, but has not been fully edited. Content may change prior to final publication. Citation information: DOI 10.1109/TSG.2018.2880654, IEEE Transactions on Smart Grid

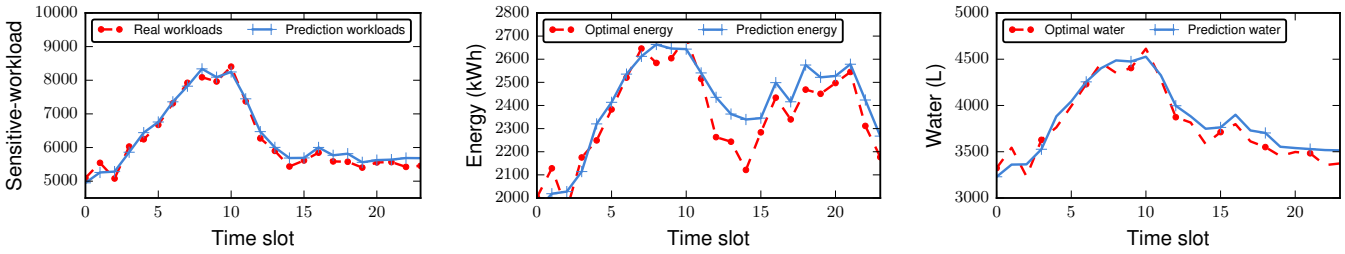

(a) Workload prediction. (b) Energy prediction. (c) Water prediction.

Fig. 13: Evaluation of the online algorithm JEWAS-ON.

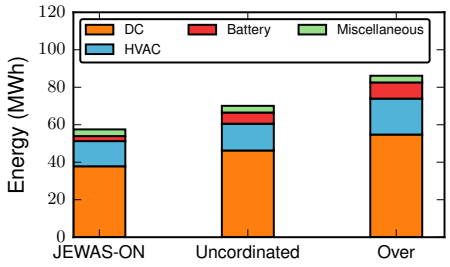

(a) Comparison among approaches.

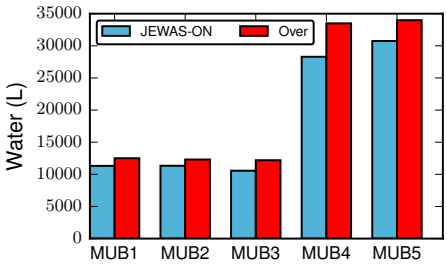

(b) Evaluation of water saving.

Fig. 14: Efficiency of energy and water saving.

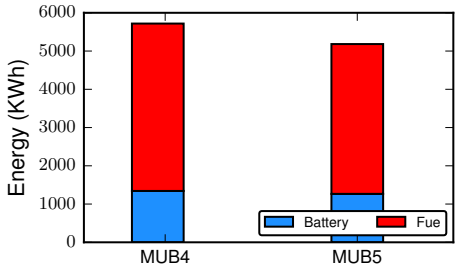

(a) Evaluation of the backup system.

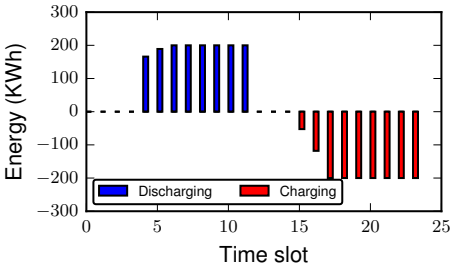

(b) Scheduling of the storage unit.

Fig. 15: Evaluation of the storage unit.

7) Effect of energy and water saving: JEWAS-ON explicitly coordinates multiple loads into its workload management decision and, by doing so, shows better results in both energy and water usage. Fig. 14 demonstrates that JEWAS-ON outperforms the others considered methods (including the uncoordinated and over-provisioning approaches) to reduce energy consumption and water usage during a daily load. The uncoordinated method is considered as the current practice; in it, the workloads are driven to the nearest datacenters without regarding other loads (offices). In addition, we consider the over provisioning benchmark as the baseline solution, in which the energy and water are supplied based on the peak load. Fig. 14a shows that our benchmark can reduce the energy consumption up to 17.39% compared to the uncoordinated approach and 33.23% compared to the over provisioning method. For another result, Fig. 14b illustrates the efficiency of water saving in all buildings compared to the over-provisioning benchmark, where it leads to a reduction of water usage up to 12.23% in all the buildings.

8) Effect of the storage unit on geo-MUBs: By considering multiple dimensions in the backup system, we show the efficiency of the storage unit factor in Fig. 15a, where the battery can achieve up to 30.66% and 32.32% amounts of power supplied by the backup system in MUB 4 and MUB 5, respectively, during 24 timeslots. The total energy supplied during 24 timeslots in our system by the backup system is shown in Fig. 15a. In this simulation, we limit the amount of energy of charging/discharging level of the battery by 200 KW, which restricts the system to exhaust the battery very quickly. In practice, with a higher storage capacity, the backup system could enhance its control capacity. Instead of merely handling the backup generator during a power shortage, the storage unit could supply a better solution to reduce the operational cost. The snapshot of charging/discharging the battery in MUB4 is shown in Fig. 15b. The storage unit plays a significant role in supplying power during peak workloads periods.

VI. Conclusion

In this paper, we have presented the way of coordinating joint energy scheduling and water saving in geo-MUBs. We have formulated an optimization problem for coupling

multiple loads (including non-datacenters and datacenters) in geographically distributed MUBs. We consider multiple knobs for energy reduction, such as IT knobs (i.e, turning on/off servers, workload management) and non-IT knobs (i.e., a cooling system, storage unit, and a fuel generator). Our model not only captures the workload management, but also concerns the impacts of office loads on datacenter loads in terms of joint energy and water management in buildings. We further consider a schedule for the system during a time horizon, where all loads can be controlled to satisfy an energy capping constraint imposed by an energy sustainability program. In order to minimize the operational cost, we apply MPC and the dual decomposition framework to address $\mathbf{P_{JEW}}$. We propose two mechanisms to be adapted for offline and online scenarios, where we can schedule the energy and water usage in buildings as well as handle the backup system. Through an extensive simulation, we show that our methods converge well in a distributed scenario. We also conducted many case studies to validate our proposed mechanisms, and in them the results reached a close-to-optimal solution.

ACKNOWLEDGMENT

This research receives support from the Canada Research Chair, Tier 1, hold by Prof. Mohamed Cheriet.

REFERENCES

[1] "Building energy data book of DOE," 2011. [Online]. Available: http://buildingsdatabook.eren.doe.gov/n

[2] N. H. Tran, C. Pham, M. Nguyen, S. Ren, and C. S. Hong, "Incentivizing energy reduction for emergency demand response in multi-tenant mixed-use buildings," *IEEE Transactions on Smart Grid*, pp. 1–1, 2016.

[3] N. H. Tran, C. Pham, S. Ren, and C. S. Hong, "Coordinated energy management for emergency demand response in mixed-use buildings," in *Ubiquitous Wireless Broadband (ICUWB), 2015 IEEE International Conference on*. IEEE, 2015, pp. 1–5.

[4] M. A. Islam, K. Ahmed, H. Xu, N. H. Tran, G. Quan, and S. Ren, "Exploiting spatio-temporal diversity for water saving in geo-distributed data centers," *IEEE Transactions on Cloud Computing*, vol. PP, no. 99, pp. 1–1, 2016.

[5] Leed certification. [Online]. Available: http://leed.usgbc.org/leed.html

[6] L. A. Barroso, J. Clidaras, and U. Hölzle, "The datacenter as a computer: an introduction to the design of warehouse-scale machines," *Synthesis Lectures on Computer Architecture*, vol. 8, no. 3, pp. 1–154, 2013.

[7] M. A. Islam, S. Ren, G. Quan, M. Z. Shakir, and A. V. Vasilakos, "Water-constrained geographic load balancing in data centers," *IEEE Transactions on Cloud Computing*, vol. 5, no. 2, pp. 208–220, April 2017.

[8] D. P. Palomar and M. Chiang, "A Tutorial on Decomposition Methods for Network Utility Maximization," *Selected Areas in Communications, IEEE Journal on*, vol. 24, no. 8, pp. 1439–1451, 2006.

[9] A. Mishra, D. Irwin, P. Shenoy, J. Kurose, and T. Zhu, "Greencharge: Managing renewableenergy in smart buildings," *IEEE J. Sel. Areas Commun.*, vol. 31, no. 7, pp. 1281–1293, Jul. 2013.

[10] M. Maasoumy, "Modeling and optimal control algorithm design for hvac systems in energy efficient buildings," 2014.

[11] T. Wei, Q. Zhu, and M. Maasoumy, "Co-scheduling of hvac control, ev charging and battery usage for building energy efficiency," in *Proceedings of the 2014 IEEE/ACM International Conference on Computer-Aided Design*. IEEE Press, 2014, pp. 191–196.

[12] S. Godo, K. Matsui, and H. Nishi, "Cost-effective air conditioning control considering comfort level and user location," in *IECON 2014 - 40th Annual Conference of the IEEE Industrial Electronics Society*. IEEE, oct 2014, pp. 5344–5349. [Online]. Available: http://ieeexplore.ieee.org/articleDetails.jsp?arnumber=7049316

[13] ASHRAE, *ASHRAE Handbook of HVAC Applications SI 2015 Edition*. ASHRAE, 2015.

[14] Reducing costs by consolidation strategies. Oracle White Paper, 2010. [Online]. Available: http://www.oracle.com/us/products/servers-storage/servers/sparc-enterprise/reducing-costs-wp-075962.pdf

[15] Y. Xiang, Z. Liu, and X. Qu, "Cpu frequency scaling algorithm for energy-saving in cloud data centers," *Journal of Software*, vol. 9, no. 9, pp. 2283–2290, 2014.

[16] Q. Wu, "Making Facebooks software infrastructure more energy efficient with autoscale," Facebook Engineering, 2014. [Online]. Available: https://code.facebook.com/posts/816473015039157/

[17] M. Lin, A. Wierman, L. L. H. Andrew, and E. Thereska, "Dynamic Right-sizing for Power-proportional Data Centers," in *Proceedings IEEE INFOCOM*, Shanghai, China, apr 2011.

[18] A. Qureshi, R. Weber, H. Balakrishnan, J. Guttag, and B. Maggs, "Cutting the electric bill for internet-scale systems," in *SIGCOMM*, 2009.

[19] Z. Chen, L. Wu, and Z. Li, "Electric demand response management for distributed large-scale internet data centers," *IEEE Transactions on Smart Grid*, vol. 5, no. 2, pp. 651–661, March 2014.

[20] N. H. Tran, C. Pham, M. N. Nguyen, S. Ren, and C. S. Hong, "Incentivizing energy reduction for emergency demand response in multi-tenant mixed-use buildings," in *GSNC16*, 2016.

[21] S. Ren, "Optimizing water efficiency in distributed data centers," in *Cloud and Green Computing (CGC), 2013 Third International Conference on*. IEEE, 2013, pp. 68–75.

[22] M. A. Islam, S. Ren, G. Quan, M. Shakir, and A. Vasilakos, "Water-constrained geographic load balancing in data centers," *IEEE Transactions on Cloud Computing*, 2015.

[23] P. Haves, B. Hencey, F. Borrell, J. Elliot, Y. Ma, B. Coffey, S. Bengea, and M. Wetter, "Model predictive control of hvac systems: Implementation and testing at the university of california, merced," Lawrence Berkeley National Lab.(LBNL), Berkeley, CA (United States), Tech. Rep., 2010.

[24] A. S. M. H. Mahmud and S. Ren, "Online resource management for data center with energy capping," in *Presented as part of the 8th International Workshop on Feedback Computing*. San Jose, CA: USENIX, 2013. [Online]. Available: https://www.usenix.org/conference/feedbackcomputing13/workshop-program/presentation/Mahmud

[25] Z. Liu, M. Lin, A. Wierman, S. Low, and L. L. H. Andrew, "Greening geographical load balancing," *IEEE/ACM Transactions on Networking*, vol. 23, no. 2, pp. 657–671, April 2015.

[26] X. Fan, W.-D. Weber, and L. A. Barroso, "Power provisioning for a warehouse-sized computer," in *ACM SIGARCH*, vol. 35, no. 2, 2007, pp. 13–23.

[27] J. M. Burgett and A. R. Chini, "Using building and occupant characteristics to predict residential residual miscellaneous electrical loads: a comparison between an asset label and an occupant-based operational model for homes in florida," *Journal of Building Performance Simulation*, vol. 9, no. 1, pp. 84–100, 2016. [Online]. Available: https://doi.org/10.1080/19401493.2014.999122

[28] R. Hendron and C. Engebrecht, *Building America house simulation protocols*. National Renewable Energy Laboratory Golden, CO, 2010.

[29] Water usage calculator. [Online]. Available: "http://spxcooling.com/green/leed/water-usage-calculator/"

[30] R. T. Marler and J. S. Arora, "The weighted sum method for multi-objective optimization: new insights," *Structural and Multidisciplinary Optimization*, vol. 41, no. 6, pp. 853–862, Jun 2010.

[31] D. P. Bertsekas, *Dynamic Programming and Optimal Control*, 2nd ed. Athena Scientific, 2000.

[32] R. Marcus and O. Papaemmanouil, "Workload management for cloud databases via machine learning," in *Data Engineering Workshops (ICDEW), 2016 IEEE 32nd International Conference on*. IEEE, 2016, pp. 27–30.

[33] N. Singh and S. Rao, "Online ensemble learning approach for server workload prediction in large datacenters," in *2012 11th International Conference on Machine Learning and Applications*, vol. 2, Dec 2012, pp. 68–71.

[34] N. Chen, X. Ren, S. Ren, and A. Wierman, "Greening multi-tenant data center demand response," in *IFIP WG 7.3 Performance*, Sydney, Australia, oct 2015.

[35] Commercial water calculator. [Online]. Available: http://www.ca.kohler.com/savewater/calculators/commercial.htm

[36] Facebook, "Open sourcing pue, wue dashboards," https://code.facebook.com/posts/272417392924843/open-sourcing-pue-wue-dashboards.